Soft Matter

Cite this: *Soft Matter*, 2011, **7**, 5566

www.rsc.org/softmatter

PAPER

Formation of colloidal assemblies in suspensions for $Pb(Mg_{1/3}Nb_{2/3})O_3$ synthesis: Monte Carlo simulation study†

Gregor Trefalt,*[a] Bosiljka Tadić[b] and Marija Kosec[a]

Received 11th February 2011, Accepted 30th March 2011
DOI: 10.1039/c1sm05228d

We study numerically the aggregation processes with three types of charged colloidal particles, PbO–lead oxide, MHC–magnesium hydroxy carbonate, and Nb_2O_5–niobium oxide, interacting in the aqueous suspensions for $Pb(Mg_{1/3}Nb_{2/3})O_3$ ceramic synthesis. Using the Monte Carlo simulations we focus on the kinetics and structure of various types of precursor clusters that may form at different pH conditions. The parameters of the interaction potentials and the particle sizes are taken to closely correspond to the experimental situations in [Trefalt *et al.*, *J. Am. Ceram. Soc.*, DOI: 10.1111/j.1551-2916.2011.04443.x, 2011], where it was shown that the pyrochlore phase, which deteriorates the electrical properties of the $Pb(Mg_{1/3}Nb_{2/3})O_3$ ceramics, results from the suspension with pH = 11.4, while the pure perovskite powder is formed when pH = 12.5. Our simulations reveal a large population of clusters with close contacts between PbO and Nb_2O_5 at pH = 11.4, which thus enable the pyroclore phase to form. Whereas, at pH = 12.5 the competition between the repulsive and the attractive interactions changes in favor of the assembly of the equilibrium clusters in which MHC particles effectively separate PbO and Nb_2O_5. We also explore how the varying size of MHC particles affects the cluster assembly at both experimentally relevant pH conditions.

1 Introduction

Lead magnesium niobate $Pb(Mg_{1/3}Nb_{2/3})O_3$ (PMN) and its solid solution with lead titanate $xPb(Mg_{1/3}Nb_{2/3})O_3$–$(1 - x)PbTiO_3$ (PMN–PT) belong to the group of perovskite relaxor ferroelectric materials. These materials are known for their large electrostrictive (strain $\sim 0.1\%$) as well as large dielectric ($\varepsilon_r \sim 13000$ at room temperature) properties and are used in actuator and high-dielectric-permittivity capacitor applications.[1–4] However, PMN and PMN–PT ceramics are difficult to prepare in the pure perovskite form.[1,2] In the conventional solid-state synthesis the reactant powders, *e.g.*, PbO, MgO, and Nb_2O_5, are homogeneously mixed and heated at elevated temperatures. The problem with this method is that two reactants PbO and Nb_2O_5 preferentially react with each-other at low temperature to form $Pb_xNb_yO_z$ pyrochlore phases. Perovskite is only formed at higher temperatures thus the synthesis usually leads to a mixture of perovskite and pyrochlore phases. Pyrochlore phases are known to deteriorate the electrical properties of PMN and PMN-PT materials,[2] therefore for obtaining high quality materials occurrence of such phases needs to be prevented during the synthesis.

We have recently proposed a novel method for the synthesis of PMN from aqueous suspensions.[5] The method enables the production of dense ceramics sintered at only 950 °C, which is about 200 K lower in comparison to conventional methods, with dielectric properties comparable to the values from the literature.[6,7]

In our method PMN is synthesized in a one step solid-state reaction. We believe this is achieved by manipulating the spatial distribution of the reagent particles in the powder mixture. In the solid-state reactions diffusion processes are the limiting factors. Specifically, for a desired reaction to occur, which leads to a new phase, it is necessary to have a close contact between the corresponding solid reactants. Hence, one can either promote or slow down certain reactions by designing of contacts, *i.e.*, spatial distribution of the reacting particles. Since the reaction between PbO and Nb_2O_5 leads to unwanted pyrochlore phases, one needs to prevent the close contacts between PbO and Nb_2O_5 particles, thus avoiding, or at least slowing down, the unwanted reactions. Therefore it is crucial to produce such spatial distributions of the reactant particles in which direct contacts between PbO and Nb_2O_5 particles are prevented in *the dried reactant powder mixtures*. In the experimental work[5] our goal is to devise the formation of precursor clusters of particles in the colloidal suspensions by controlling the interactions between the reagent particles, which is achieved by controlling the pH of the suspension.

By changing the suspension pH, the surface charge of the colloidal particles is altered and consequently the electrostatic

[a]*Electronic Ceramics Department, Jožef Stefan Institute, Jamova 39, 1000 Ljubljana, Slovenia. E-mail: gregor.trefalt@ijs.si*
[b]*Department of Theoretical Physics, Jožef Stefan Institute, Jamova 39, 1000 Ljubljana, Slovenia*

† Electronic supplementary information (ESI) available. See DOI: 10.1039/c1sm05228d

interactions between the particles are changed. From zeta-potential measurements[5] (see Fig. 1) we predict the electrostatic interactions between our reagent particles, namely PbO, Nb_2O_5, and magnesium basic carbonate (MHC). Two pH conditions are considered: (*i*) pH = 11.4, which is inherent pH of the suspension of the powder mixture, and (*ii*) pH = 12.5. At pH = 11.4, where $\zeta_{PbO} = +40$ mV and $\zeta_{Nb_2O_5} = -80$ mV, thus due to opposite sign of ζ potentials, the electrostatic attraction between PbO and Nb_2O_5 is expected, while $\zeta_{MHC} = +20$ mV. At pH = 12.5, on the other hand, $\zeta_{PbO} = -50$ mV, $\zeta_{Nb_2O_5} = -100$ mV, and $\zeta_{MHC} = 20$ mV, now repulsive electrostatic interaction is expected between PbO and Nb_2O_5, and attractive interaction between PbO and MHC, and Nb_2O_5 and MHC, respectively. Based on the zeta-potential measurements we propose the following hypothesis. The electrostatic interactions in the suspension with pH = 11.4 should promote the formation of clusters with close contacts between PbO and Nb_2O_5 particles, as schematically presented in Fig. 1b. On the contrary, at pH = 12.5 colloid–colloid interactions may lead to clusters in which close contacts between PbO and Nb_2O_5 particles do not occur while MHC particles are interacting with both PbO and Nb_2O_5 particles, also shown Fig. 1b. We propose that the structure of the as-formed colloidal assemblies, that occur at different pH suspensions, has a key influence on the solid-state reactions.[5] We assume that the same spatial distributions of the particles remains in the dried powders.

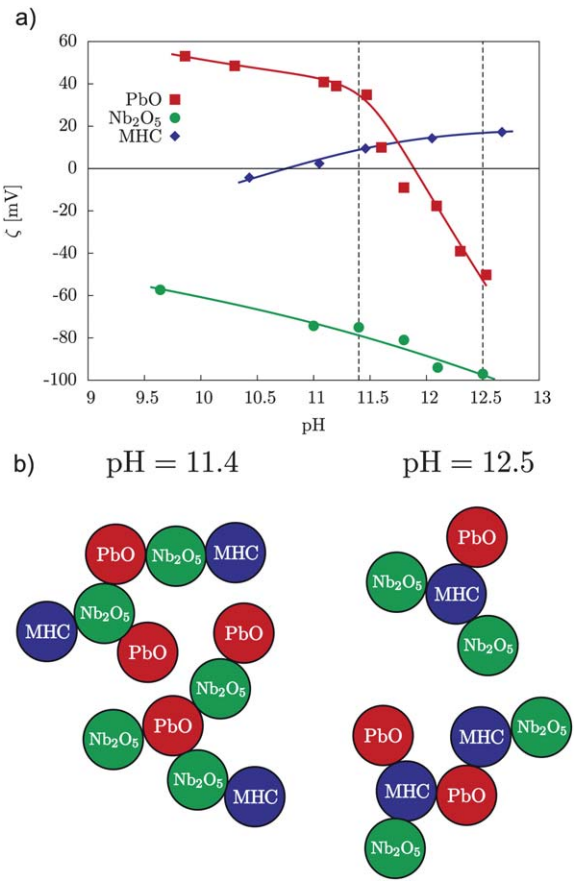

Fig. 1 a) Measured zeta-potentials of PbO, Nb_2O_5 and MHC particles as a function of the suspension pH. The two pH conditions considered in experiment and simulations are denoted by dashed lines. b) Schematic presentation of the predicted cluster formation in the suspensions with pH = 11.4 and pH = 12.5.

Our experimental results show[5] that after the solid-state synthesis pure perovskite powders are obtained from the pH = 12.5 suspension, whereas the powders obtained from the pH = 11.4 suspensions contain pyrochlore phase in addition to the perovskite. However, the structure of the aggregates in the suspension is hard to investigate experimentally. Here we address the problem of formation of the precursor clusters with the numerical simulations using the Monte Carlo method with realistic potentials.

For the calculation of interactions in the system of charged colloidal particles the Derjaguin–Landau–Verwey–Overbeek (DLVO) theory is widely used.[8–12] According to DLVO theory, the pair potentials consist of the electrostatic and van der Waals interactions. Hence, the aggregates are formed in the competition between the attractive and the repulsive interactions. Moreover, in the multicomponent systems a combination of the direct and indirect interactions stemming from other particles in the suspension, affects the process, making the prediction of the assembly even more complicated. Here usually numerical simulations are employed to model the particle ensembles. Brownian Dynamics method and Monte Carlo simulation techniques[11,13–18] are among widely used methods in this field. In the study of aggregation processes with colloidal-cluster formation, Monte Carlo (MC) simulations are efficient in terms of performance. The results reported in recent studies by MC simulations are shown to be in agreement with experimental findings and theoretical predictions.[19–22] In this work we use Monte Carlo simulations to study the assembly of small precursor clusters of charged colloidal particles of the reagent powders PbO, MHC, and Nb_2O_5 in the suspensions for PMN synthesis and to elucidate the role of pH in the aggregation processes. With the close reference to the experimental situations we would like to complement the experimental results in ref. 5 by providing the underlying picture of the assembly processes at microscopic scale, and to explore a wider range of parameters, that might be interesting for future experiments.

2 Experimental system

The experimental procedures and the results are in detail explained in our previous work.[5] Here we briefly present the experimental results that are either used as input parameters for the simulations or are relevant to the results of numerical simulations.

2.1 Sample preparation

Aqueous suspensions of PbO (99.9%, Sigma Aldrich), $(MgCO_3)_4Mg(OH)_2{\cdot}4H_2O$ (41.91% of MgO, determined by thermogravimetric analysis, Sigma Aldrich), and Nb_2O_5 (99.9%, Sigma Aldrich) powders are prepared containing 20 wt.% of solid load in total. The powders are mixed in molar ratio corresponding to the stoichiometry of PMN. Two sets of experiments are performed: (*i*) suspensions with starting pH = 11.4, the inherent pH of suspension, and (*ii*) suspensions with starting pH = 12.5, adjusted by the aqueous ammonia solution (25 wt.%,

Merck), the samples will be further denoted as pH 11.4, and pH 12.5 sample, respectively. After the pH adjustment both suspensions are milled in an attrition mill for 3 h with 800 rpm, using 3 mm yttria-stabilized zirconia balls, and subsequently dried at 100 °C. The dried powders are heated to 900 °C with the rate 2 K min^{-1} and kept at this temperature for 5 h. At this step the solid-state reaction takes place.

2.2 Characterization

The zeta-potentials (ζ) of reagent powders are measured as a function of the suspension pH by electrophoretic light scattering technique (BI Zeta PALS MAS instrument, Brookhaven Instruments Corp.). The concentration of the powders is kept at 0.05 wt.%, the pH is adjusted by HCl (aq) and NaOH (aq) solutions. We observed that the pH adjustment with the ammonia solution yielded the same results. The results are presented in Fig. 1. The two pH conditions considered in experiment and simulations are denoted by dashed lines.

The size of the particles in the milled powder mixtures is determined by static light scattering technique using Microtrac S3500 instrument. The particle size distributions in both dried samples are narrow with similar average sizes of particles equal to 0.42 μm and 0.40 μm for pH 11.4 and pH 12.5 samples, respectively. The average measured particle sizes are used as input parameters for the simulations. Notice that the particle sizes are measured in the suspension mixture of PbO, Nb_2O_5, and MHC particles, therefore within the experimental procedure we cannot distinguish between the sizes of different types of particles. In principle, sizes of each type of particles can be measured by separate milling of their powders. However, this may lead to different results, due to changed conditions to which the particles are exposed, compared to the conditions when the mixture is milled, as in the experiment. However, in the simulations we consider both situations: equal sizes of all type of particles as well as a choices of different sizes of MHC particles, which may affect the assembly processes at most. Morphology of the powders is examined by field emission scanning electron microscope FE-SEM SUPRA 35 VP, Carl Zeiss (Fig. 2). Both samples consist of sub-micrometre particles. The morphology and sizes of the particles are similar in both cases. Obviously the pH conditions do not influence the size and morphology of the milled powder mixtures.

3 Model and simulation method

3.1 Model

We consider the model of the interacting charged colloidal particles within a suitable potential and the parameters selected such that they match closely the experimental system in ref. 5. Three-component system is used in the simulations, representing three types of charged particles in the experiment, PbO, MHC, and Nb_2O_5. As explained in detail below, the model parameters are either extracted from the experiment[5] or otherwise taken from the literature to closely mimic the experimental conditions.[5]

The coarse grained model is employed. The particles in the suspensions are assumed to be charged hard spheres in a continuous medium. Water molecules and ion species in the suspension are not modeled explicitly, only their average

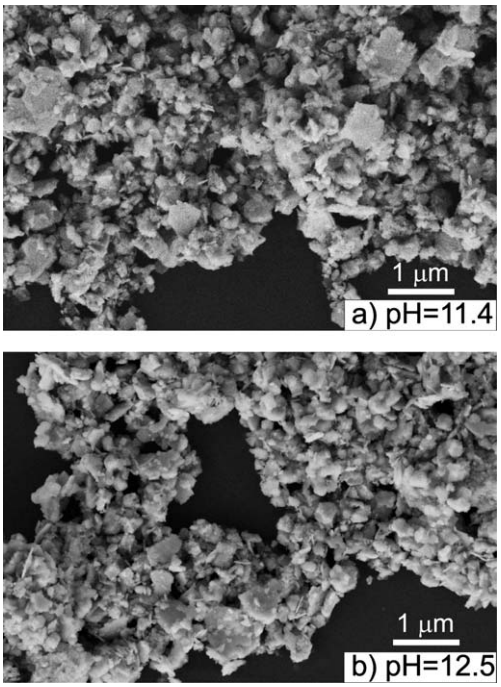

Fig. 2 FE-SEM micrographs of the dried powder mixtures for a) pH 11.4 and b) pH 12.5 samples. In both samples sub-micrometre particles are observed, which is in agreement with the light scattering measurements.[5]

contribution on the colloid–colloid interactions is taken into account. As mentioned in the introduction, the DLVO[23,24] potential is suitable to model interactions in these systems. According to the theory, the pair potential U_{ij}^{DLVO} between the colloidal particles i and j is composed of the electrostatic contribution, U_{ij}^{el}, and the van der Waals contribution, U_{ij}^{vdW}. In our case the hard-core interaction, U_{ij}^{hc}, is added to prevent the overlapping of the particles. For each pair (ij) of the reagent particles we have:

$$U_{ij}^{\mathrm{DLVO}} = U_{ij}^{\mathrm{vdW}} + U_{ij}^{\mathrm{el}} + U_{ij}^{\mathrm{hc}}. \quad (1)$$

For van der Waals interaction the following expression for spherical particles is used,[25]

$$U(r_{ij}) = -\frac{A_{ij}}{6}\cdot\left[\frac{2a_ia_j}{r_{ij}^2-(a_i+a_j)^2} + \frac{2a_ia_j}{r_{ij}^2-(a_i-a_j)^2}\cdot\ln\left(\frac{r_{ij}^2-(a_i+a_j)^2}{r_{ij}^2-(a_i-a_j)^2}\right)\right], \quad (2)$$

where A_{ij} is the Hamaker constant, r_{ij} is the center to center distance, and a_i and a_j are the radii of the interacting particles. The Hamaker constant depends on the material from which the particles are composed and the medium through which they interact. Typical values of the Hamaker constants in the case of the particles of inorganic materials interacting through water are in the range of 1×10^{-21} to 1×10^{-19} J.[26] However, we did not find in the literature the exact values of A_{ij} for the materials used in our experiments, *i.e.*, PbO, Nb_2O_5, MHC, therefore all Hamaker constants in our simulations are chosen to be equal to $A = 3 \times 10^{-20}$ J.

Hogg–Healy–Furstenau (HHF) equation is used for calculation of the electrostatic interactions:[27]

$$U_{ij}^{\mathrm{el}} = \pi\varepsilon_{\mathrm{r}}\varepsilon_0 \cdot \frac{a_i a_j}{a_i + a_j}\Big[\left(\psi_i + \psi_j\right)^2 \ln\left(1 + e^{-\kappa h}\right) + \left(\psi_i - \psi_j\right)^2 \ln\left(1 - e^{-\kappa h}\right)\Big], \quad (3)$$

where $h = r_{ij} - (a_i + a_j)$ is the surface-to-surface distance between the particles, $\varepsilon_{\mathrm{r}}\varepsilon_0$ is the dielectric permittivity of the medium, ψ_i is the electrostatic surface potential of the particle i, and κ is the inverse Debye screening length. For dielectric constant, the value for water is used $\varepsilon_{\mathrm{r}} = 78.5$. The electrostatic surface potential values are taken from the zeta potential measurements,[5] see Fig. 1a. The values for the Debye screening length are calculated from the estimated ion concentrations. Because relatively high pH = 11.4 and 12.5 values are used in our experiment, assuming that the major contribution to the ion concentration comes from the OH^- ions and their counter-ions is reasonable. Therefore the ion concentration can be estimated from the pH. The ionic strength $I = \sum_i c_i z_i$ is calculated from the ion concentration c_i, and z_i is the charge number of the ion. The Debye length which is used in the simulations is then calculated as:

$$\kappa = \sqrt{\frac{2N_{\mathrm{A}}e^2 I}{\varepsilon_0\varepsilon_{\mathrm{r}}kT}} = 1.6 \times 10^8\ \mathrm{m}^{-1}, \quad (4)$$

where N_{A} is the Avogadro number, e the elementary charge, and I is the ionic strength.

The third term in the eqn (1) describes the hard–core interaction. In this case the interaction energy is zero for non-overlapping particles and infinite for distances where the particles would overlap:

$$U_{ij}^{\mathrm{hc}} = \begin{cases} \infty; & r_{ij} \le \dfrac{a_i + a_j}{2} \\ 0; & r_{ij} > \dfrac{a_i + a_j}{2}. \end{cases} \quad (5)$$

The cutoff distance for all the potentials is equal to $r_{\mathrm{cutoff}} = 2.2(a_i + a_j)$. At this distance the interaction energy is practically zero.

Numerical values of all the parameters for the interaction potential used in our simulations are summarized in Tables 1 and 2.

3.2 Simulation method

To simulate the aggregation processes with these three types of charged particles in the aqueous suspension we use the three-dimensional off-lattice Monte Carlo technique at finite temperature.[15,16,20,28] The canonical ensemble with the fixed number of particles N, volume V, and temperature T is used. The temperature is fixed to $T = 293$ K and the total number of particles in the simulation cell is 100 in all cases, except in the case of larger MHC particles, where 200 particles in total are used. The cubic simulation cell with the periodic boundary conditions and the minimum image convention are employed.[16] The volume of the simulation cell is calculated from the volume concentrations (ϕ) of the particles and the number of the particles in the simulation cell. In all simulations we keep the concentrations of the particles the same as in the experiments, *i.e.*, $\phi_{\mathrm{PbO}} = 1.6$ vol.%, $\phi_{\mathrm{Nb_2O_5}} = 1.2$ vol.%, and $\phi_{\mathrm{MHC}} = 1.0$ vol.%, respectively.

Within the MC technique, the aggregation process, in which the interacting particles diffuse towards energetically stable positions, is considered in the configurational space. The starting configuration of the particles is chosen randomly with the condition that their mutual distances are larger than $r_{ij} = 1.2(a_i + a_j)$, where the interaction energy is almost zero. Then at each MC step a random particle is chosen and moved to a new position by a small random displacement Δr, which is chosen from $[0, \Delta r_{\max}]$ interval using uniform random numbers. The difference in the energy of the system on-going from one state to another state, ΔE, is calculated *via* the expressions in eqn (1), (2), (3, 5) summed over all pairs of particles. The attempted move is accepted if the transition probability

$$P = e^{-\frac{\Delta E}{kT}} \ge \eta, \quad (6)$$

exceeds a random number $\eta \in [0,1]$, otherwise the new configuration is rejected. Then another particle is selected randomly and attempted to move, and so on. These steps are cycled until the system reaches the equilibrium.

To validate the results, test simulations with a larger number of particles are carried out. To check the reproducibility of the equilibrium states, the simulations with the same parameters but different initial configuration of the particles are carried out. Reproducible results are obtained. In each case the actual

Table 1 Parameters for the interaction potential: reagent particles of equal size

pH	$a_{\mathrm{PbO}} = a_{\mathrm{Nb_2O_5}} = a_{\mathrm{MHC}}$	ψ_{PbO}	$\psi_{\mathrm{Nb_2O_5}}$	ψ_{MHC}	A_{ij}	κ
11.4	200 nm	40 mV	−80 mV	10 mV	3×10^{-20}J	1.6×10^8m^{-1}
12.5	200 nm	−50 mV	−100 mV	20 mV	3×10^{-20}J	1.6×10^8m^{-1}

Table 2 Parameters for the interaction potential: different reagent particle sizes

pH	$a_{\mathrm{PbO}} = a_{\mathrm{Nb_2O_5}}$	a_{MHC}	ψ_{PbO}	$\psi_{\mathrm{Nb_2O_5}}$	ψ_{MHC}	A_{ij}	κ
Smaller MHC particles (a_{PbO}, $a_{\mathrm{Nb_2O_5}} : a_{\mathrm{MHC}} = 2 : 1$)							
11.4	200 nm	100 nm	40 mV	−80 mV	10 mV	3×10^{-20} J	1.6×10^8 m^{-1}
12.5	200 nm	100 nm	−50 mV	−100 mV	20 mV	3×10^{-20} J	1.6×10^8 m^{-1}
Bigger MHC particles (a_{PbO}, $a_{\mathrm{Nb_2O_5}} : a_{\mathrm{MHC}} = 1 : 2$)							
11.4	100 nm	200 nm	40 mV	−80 mV	10 mV	3×10^{-20} J	1.6×10^8 m^{-1}
12.5	100 nm	200 nm	−50 mV	−100 mV	20 mV	3×10^{-20} J	1.6×10^8 m^{-1}

number of the Monte Carlo steps is $N_{step} = 2 \times 10^9$. Note that such large number of steps is needed to reach the equilibrium because small displacements $\Delta r_{max} = 1$ nm need to be applied, in view of the small range of the DLVO potentials (see Fig. 3). Large steps Δr can lead to jumps over the potential maximum and hence to unphysical results. The maximum displacements used in the simulations are below 0.04% of a cell length, $\Delta r < 0.0004 \cdot \ell_{cell}$. To mimic the experimental situation we also keep the room temperature throughout the simulations. In this way we allow that a particle, which is already bound to a cluster, may drift away due to favorable thermal fluctuations. The energy of the system steadily decreases with the simulation time before it levels up for large times (in the Electronic Supplementary Information the energy plotted against time is shown for all cases studied in this paper).† The attractive interaction potentials are very steep when the particles are close to each other, resulting in an large negative energies in comparison to $k_b T$, see for instance Fig. 3a. Therefore in most cases the cluster fragmentation is not energetically favorable. On the other hand, the clusters themselves are not fixed in space. They evolve through the individual particle dynamics-addition or detachment of the particles, and their centers of mass move. For the objectives of this work explained above, we are mainly focused to the inner structure of these clusters. The interesting cluster–cluster aggregation processes and large-scale structures[17] that may emerge are left out of this paper.

4 Emergent clusters of three types of charged particles in suspensions

In this section we present the results of the MC simulations. For comparison of the two samples, representing the pH = 11.4 and pH = 12.5 suspensions, the simulation results are systematically plotted side by side. In each case, first the interaction potentials between the charged particles PbO, MHC, and Nb_2O_5 are calculated with the use of eqn (2) and (3). As already described above, the parameters which can be measured, are inferred from the

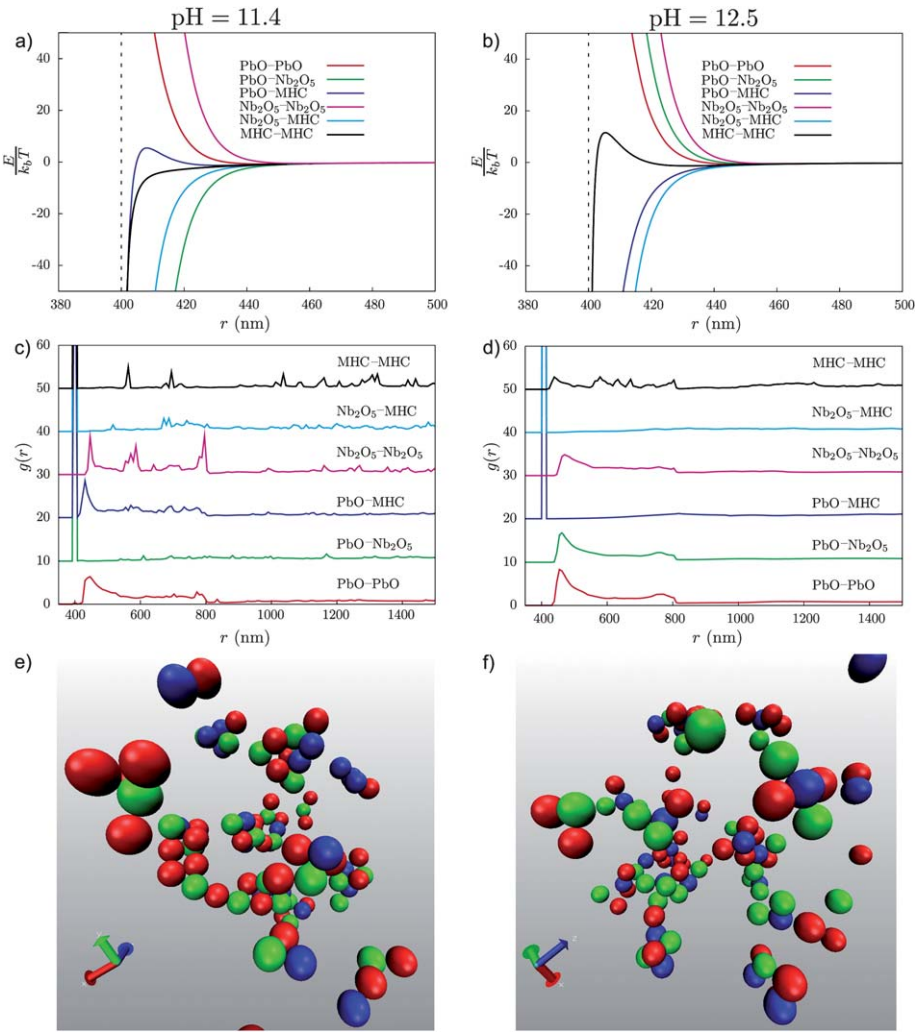

Fig. 3 Results for the reagent particles of equal size. (a and b) Interaction potentials between six pairs of particles in the suspension. (c and d) Simulated radial distribution functions for the pairs of particles, as indicated. (e and f) Snapshots of the equilibrated spatial distribution of particles in the suspensions, PbO is colored red, Nb_2O_5 green, and MHC blue. Perspective 3D views are generated with VMD program.[29] The results for the pH 11.4 sample are presented on the left and for the pH 12.5 sample on the right.

experiment,[5] and the remaining parameters are taken from the literature to mimic the corresponding experimental conditions.

4.1 Reagent particles of equal size

We first perform simulations assuming that all three types of the particles have equal sizes. The diameter of the reagent particles is taken as 400 nm, which corresponds to the average size of the particle mixture in the suspension, measured with the static light scattering in both pH 11.4 and pH 12.5 samples. The set of all parameters used for the calculations is given in Table 1. The effects of different sizes of the reacting particles are considered in the following section. In Fig. 3a and 3b the computed interaction potentials for the pH 11.4 and pH 12.5 samples are shown, respectively. Six different pair interactions are present in the three component system. All interactions are short-ranged as they decay to zero already at around 450 nm, while the contact distance of the particles is 400 nm. In the case of pH = 11.4, the interactions between PbO–PbO, Nb_2O_5–Nb_2O_5, and PbO–MHC are repulsive, with the PbO–MHC interaction reaching the maximum of only 5 k_bT. These pairs of particles possess the zeta potential of the same sign, therefore in all cases the electrostatic interaction is repulsive and stronger in comparison to the attractive van der Waals interaction, leading to a positive sum of both contributions. The other three interactions, *i.e.*, PbO–Nb_2O_5, Nb_2O_5–MHC, and MHC–MHC, are attractive. The latter pair has the same sign of the charge on the surface of both particles, therefore electrostatic interaction is repulsive, but due to the small value of $\zeta = 10$ mV the van der Waals attraction prevails, thus the sum is negative. The PbO–Nb_2O_5 and Nb_2O_5–MHC pairs possess the opposite sign of ζ, therefore both electrostatic and van der Waals interactions are negative leading to the attractive potential. At pH = 12.5 case, however, the PbO–Nb_2O_5, PbO–MHC, and MHC–MHC interactions change due to the change in zeta potentials (*cf.* Table 1 and Fig. 1). In this case, PbO–Nb_2O_5 and MHC–MCH interactions become repulsive, whereas the PbO–MHC interaction is attractive. Hence, comparing the two pH conditions, apart from the numerical values, the main difference appears in the PbO–Nb_2O_5 interaction, which is attractive at pH = 11.4, and repulsive at pH = 12.5.

The calculated interactions are then used in the simulations. As discussed in the Introduction, our main focus here is on the spatial distribution of the reagent particles and formation of their clusters in the suspensions. Therefore the main simulation results concern the radial distribution functions (RDFs), which are computed for all pairs of particles, as well as the snapshots of equilibrium distributions of the particles emerging after a long simulation time. The results are presented in Fig. 3c to 3f for both pH 11.4 and pH 12.5 samples. In Fig. 3c and 3d the radial distribution functions $g(r)$ for the pairs of particles are presented. For clarity, the curves are systematically shifted upwards by 10 units. As both Fig. 3c and 3d show, the length at which the perturbations in the RDFs are observed, is at least twice the range of the interaction potentials, which can be attributed to indirect interactions between these particles.

In pH 11.4 case, the RDFs can be divided in two groups: (*i*) the functions for PbO–Nb_2O_5, PbO–MHC, Nb_2O_5–MHC, and MHC–MHC radial distributions have a large sharp peak at 400 nm, which means that these pairs of particles are in close contact (note that the closest approach is equal to the particle diameter 400 nm); (*ii*) in the RDFs of PbO–PbO and Nb_2O_5–Nb_2O_5 pairs, the first peak is observed at 450 nm. Moreover, the Nb_2O_5–Nb_2O_5 RDF includes three larger peaks observed at 450, 600, and 800 nm, whereas the PbO–PbO function has one diffusive peak ranging from 450 to 800 nm. From the RDF shapes we conclude, that the PbO adsorbs to the surface of Nb_2O_5 particles, thus the distances between two PbO particles adsorbed to Nb_2O_5 can be from 450 to 800 nm (an illustration is shown in Fig. 4). This explains the occurrence of the diffusive peak from 450 to 800 nm in the RDF of the PbO–PbO pair. These shapes of the RDFs are in agreement with the equilibrium configuration of the particles presented in Fig. 3e, where the PbO particles are colored red, the Nb_2O_5 particles green, and the MHC particles blue. Clusters with close contacts between PbO and Nb_2O_5 particles are visible, while the spatial distribution of MHC particles is inhomogeneous.

In the pH 12.5 case, again two types of the RDFs can be distinguished, Fig. 3d: the RDFs with a large sharp peak at 400 nm, for the PbO–MHC and Nb_2O_5–MHC functions, and the RDFs with a diffusive peak ranging from 450 to 800 nm, for the PbO–PbO, PbO–Nb_2O_5, Nb_2O_5–Nb_2O_5, and MHC–MHC functions. Direct contacts between the PbO–MHC and Nb_2O_5–MHC pairs, together with the diffusive shape of PbO–PbO, PbO–Nb_2O_5, and Nb_2O_5–Nb_2O_5 RDFs, could be explained with the adsorption of PbO and Nb_2O_5 particles on MHC particles. The adsorption of PbO and Nb_2O_5 on MHC particles is also seen in Fig. 3f. Again PbO is colored red, Nb_2O_5 green, and MHC blue. In agreement with the RDFs, the spatial distribution of the particles reveals the clusters where PbO and Nb_2O_5 particles are separated by MHC particles, and the distribution of MHC particles is more homogeneous.

Our simulation results reveal that the formation of colloidal clusters in the two samples is different. In particular, in contrast to the pH 11.4 suspension, the close contacts between PbO and Nb_2O_5 are not seen in the pH 12.5 sample. These findings are confirmed both by the absence of a sharp peak in the PbO–Nb_2O_5 RDF at the contact distance 400 nm, and by visual inspection of the equilibrium cluster structures. While the clusters with close contacts between PbO and Nb_2O_5 particles are observed in the pH11.4 suspension, such clusters are absent in the pH12.5 sample, where the close contacts between PbO and Nb_2O_5 are prevented by the MHC particles. Consequently the distribution of the MHC particles is more homogeneous in the pH 12.5 suspension in comparison to the pH 11.4 suspension.

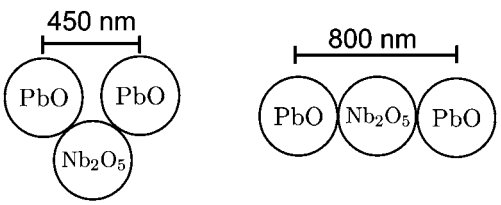

Fig. 4 Schematic presentation of two PbO particles adsorbed on the Nb_2O_5 particle. The closest distance between two PbO particles is at 450 nm (repulsive potential), left configuration, and the largest at 800 nm, right configuration.

The results of the simulations are in agreement with our experimental findings. In the pH 11.4 sample the simulations reveal formation of the clusters with close contacts between PbO and Nb_2O_5 particles and uneven distribution of the MHC particles. This situation is favorable for the formation of secondary pyrochlore phase, which is found in the experiments.[5] Contrary to the pH 11.4 case, such type of clusters are not present in the pH 12.5 sample, where the MHC particles prevent direct contacts between PbO and Nb_2O_5 particles in the equilibrium clusters. Thus after heating the sample, only the perovskite phase can be formed, as also found in the experiment. Close inspection of the simulated structure of aggregates at pH 11.4 and pH 12.5 samples, with example snapshots shown in Fig. 3e and 3f, confirms two different types of clusters of the reagent powders, depicted in Fig. 1b, as anticipated on the basis of the experimental results.

4.2 Particle size effects

In this section we further studied the influence of the size of the particles on the cluster formation at both pH = 11.4 and pH = 12.5 conditions. The particle sizes affect the interaction potentials in eqn (2), (3) and (5). Hence the geometry of the emergent clusters may change and consequently the physical properties of the aggregates. Examples of such aggregation processes with two neutral colloidal particles of different sizes are studied in connection with the assembled nanoparticle films.[17] In the present case, the situation is more complex: apart from the geometric effects, we have three types of charged colloidal particles, whose ζ-potentials are different. The MHC particles play the crucial role in the prevention of the pyrochlore phase by blocking the contacts between the PbO and Nb_2O_5 particles, as shown in the previous section. Here we examine how the size of the MHC particle can affect the process of the cluster formation. In the simulations we assume that the size of the MHC particles is reduced to 200 nm in one case (smaller MHC particles) and in the other we reduce the sizes of both PbO and Nb_2O_5 particles to 200 nm (bigger MHC particles). All other parameters remain the same as in the case with equal-sized reagent particles. The summary of all parameters is given in Table 2.

The results of the simulations for the pH 11.4 and pH 12.5 samples with smaller MHC particles are presented in parallel in Fig. 5. Due to the smaller size of the MHC particles the closest approaches of the particle pairs are now found at three different distances, beyond which the interaction range extends. These are the following distances: 200 nm (MHC–MHC pair), 300 nm (PbO–MHC and Nb_2O_5–MHC pairs), and 400 nm (PbO–PbO, PbO–Nb_2O_5, Nb_2O_5–Nb_2O_5 pairs), respectively. The computed interaction potentials for the pH 11.4 sample are shown in Fig. 5a. Three repulsive interactions, *i.e.*, between the PbO–PbO, Nb_2O_5–Nb_2O_5, PbO–MHC pairs are found, while three attractive interactions are for the PbO–Nb_2O_5, Nb_2O_5–MHC, and MHC–MHC pairs of particles.

Likewise as in the case of equal-sized particles studied above, at the pH 12.5 sample, shown in Fig. 5b, the nature of three interactions is altered in comparison with the pH 11.4 sample, due to the changes in the zeta potentials. Namely, the interactions PbO–Nb_2O_5 and MHC–MHC change from the attractive to the repulsive, while PbO–MHC interaction changes from the repulsive to the attractive. As shown below, the altered nature of the PbO–Nb_2O_5 interaction is crucial in this case for the cluster formation.

The simulated RDFs for the pairs of particles in the pH 11.4 suspension are presented in Fig. 5c. Again, two groups of the functions are readily distinguished. One group comprises the RDFs with sharp peaks at the distance corresponding to the closest approach of two particles, as found for the PbO–Nb_2O_5, PbO–MHC, Nb_2O_5–MHC, MHC–MHC pairs. The other group consists of the functions, where the peaks at the distance of closest approach are absent, as found for the PbO–PbO and Nb_2O_5–Nb_2O_5 pairs. From the RDFs and the equilibrium distribution of the particles in suspension, which is shown in Fig. 5e, it can be seen that not only the clusters of PbO and Nb_2O_5 are formed, but also the clusters of MHC particles are present. When the MHC particles form clusters by themselves, they do not adsorb to the surfaces of PbO and Nb_2O_5, and consequently can not prevent their direct contacts. Such situation leads to a non-homogeneous distribution of MHC particles and the clusters with close contacts between PbO and Nb_2O_5 particles.

The situation is different in the pH 12.5 sample, the respective RDFs and equilibrium distributions of particles are presented in Fig. 5d and f. Three types of RDFs are found in the pH 12.5 suspension. PbO–PbO, PbO–Nb_2O_5, and Nb_2O_5–Nb_2O_5 functions contain several peaks at distances larger than the distance of their closest approach. This implies that there are no direct contacts between these pairs of particles. The RDFs for the PbO–MHC and Nb_2O_5–MHC pairs exhibit just one large sharp peak at the distance of the closest approach, indicating that practically all MHC particles are adsorbed to the PbO and Nb_2O_5 surfaces. This is further confirmed with the shape of the MHC–MHC RDF, where in addition to the peak at their closest approach at 200 nm, also a diffusive peak from 200 nm to 600 nm is observed, which indicates adsorption of MHC particles to the other two components. The snapshot of the equilibrium distribution of the particles, shown in Fig. 5f, reveals that practically all MHC particles are adsorbed to either PbO or Nb_2O_5. Although the clusters containing all three components form, the direct contact between PbO and Nb_2O_5 is always prevented by the MHC particles. Therefore by increasing the pH to 12.5 we are able to achieve a homogeneous distribution of the MHC particles which at the same time prevent direct contacts between PbO and Nb_2O_5 particles.

Similar as in the case with equal-sized reagent particles, we can conclude that colloidal assemblies formed at pH = 12.5 are more favorable for the synthesis of the single phase perovskite PMN in comparison to the pH = 11.4 conditions.

The results for the system with bigger MHC particles are presented in Fig. 6. Due to the differences in the actual sizes of the particles, the distances of their close contacts are changed as follows: for PbO–PbO, PbO–Nb_2O_5, and Nb_2O_5–Nb_2O_5 the interactions start at 200 nm, PbO–MHC and Nb_2O_5–MHC at 300 nm, and MHC–MHC at 400 nm. Apart from the different distances, the nature of the potentials remains the same as in the case of smaller MHC particles. At pH = 11.4, the potentials between the PbO–PbO, Nb_2O_5–Nb_2O_5, PbO–MHC pairs are attractive, whereas the repulsive potentials exist between the PbO–Nb_2O_5, Nb_2O_5–MHC, and MHC–MHC pairs. At pH =

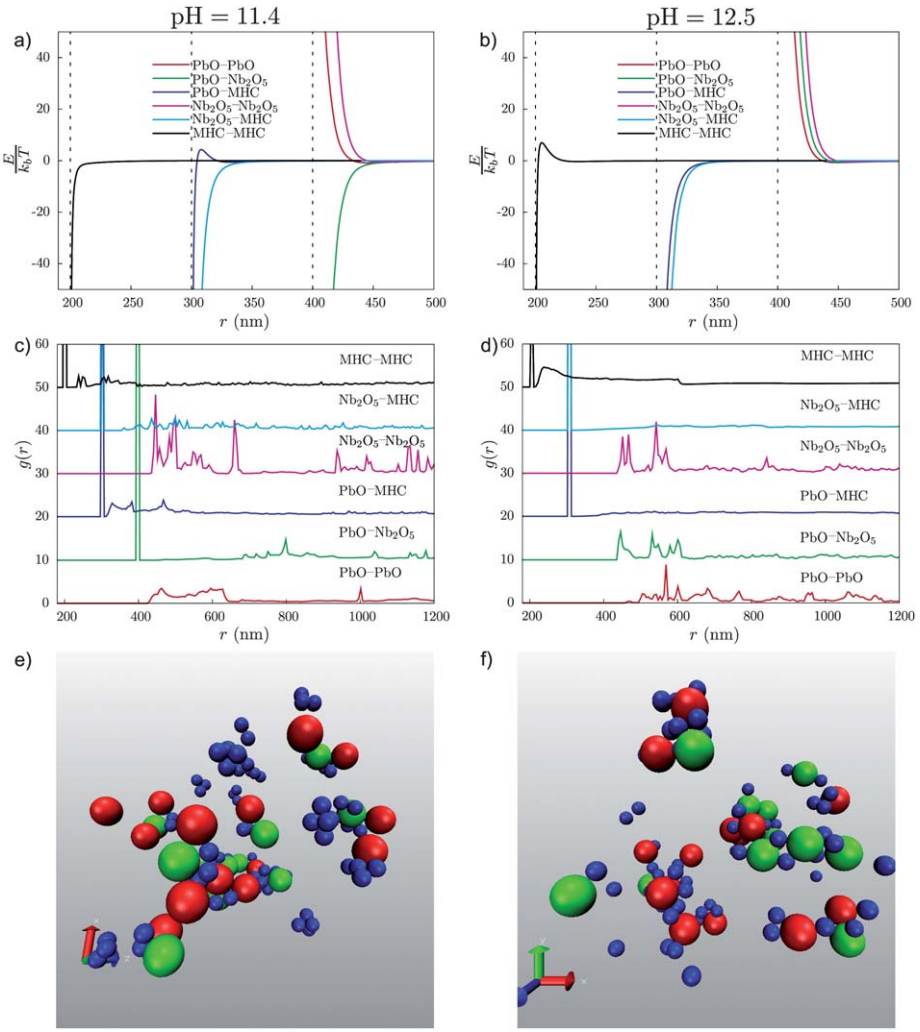

Fig. 5 Results for the smaller MHC particles. (a and b) Interaction potentials between six pairs of particles in the suspension. (c and d) Simulated radial distribution functions for the pairs of particles. (e and f) Snapshots of equilibrated spatial distribution of particles in the suspensions. As above, the PbO particles are colored by red, Nb_2O_5 green, and MHC blue. The perspective 3D views are generated with VMD program.[29] The results for the pH 11.4 sample are presented on the left and for the pH 12.5 sample on the right.

12.5, on the other hand, the interactions between PbO–Nb_2O_5 and MHC–MHC are repulsive, and the PbO–MHC interaction is attractive, for the reasons already explained above.

In Fig. 6c and 6e the computed RDFs for different pairs and a snapshot of equilibrium distributions of particles at pH = 11.4 are presented. We can observe the formation of worm-like clusters of PbO and Nb_2O_5 particles, and the presence of clusters are confirmed with the peak in PbO–Nb_2O_5 RDF at the distance of closest approach. The PbO and Nb_2O_5 particles are also partly adsorbed on MHC particles which is also seen from the peaks of PbO–MHC and Nb_2O_5–MHC RDFs. Similarly to both previous cases, at pH = 11.4, here we also observe a large number of direct contacts between PbO and Nb_2O_5 particles, which are not desired for the synthesis.

In Fig. 6d and 6f the results for pH = 12.5 conditions and larger MHC particles are presented. Similarly as in the case with equal-sized reagent particles, the diffusive peaks in the PbO–PbO, PbO–Nb_2O_5, and Nb_2O_5–Nb_2O_5 RDFs are observed, while the sharp peaks at the distance of the closest approach in PbO–MHC and Nb_2O_5–MHC RDFs are seen. From these results and also from the spatial distribution of particles, we can conclude that PbO and Nb_2O_5 particles are adsorbed on MHC particles and that direct contacts between PbO and Nb_2O_5 particles are effectively prevented. However, from Fig. 6f it can be observed, that not all the PbO and Nb_2O_5 particles are adsorbed on MHC particles. To quantify the adsorption, the amount of isolated PbO and Nb_2O_5 particles is calculated. About 43% of PbO and Nb_2O_5 particles are adsorbed to the MHC particles, which leaves 57% of them isolated. From the point of view of solid-state reaction, only partial adsorption of PbO and Nb_2O_5 particles is not beneficial. Although we do not have direct contacts between PbO and Nb_2O_5 particles in the suspension, the situation can change during the drying process. Firstly during drying the screening length κ is increasing, due to the increase of the ion concentration, and consequently the van der Weals forces become dominant. This could lead to attractive potential between PbO and Nb_2O_5. Secondly, additional attraction between these particles may also be caused by capillary forces. Having more than 50% of PbO and Nb_2O_5 particles unabsorbed, we can expect that a number of them may get in

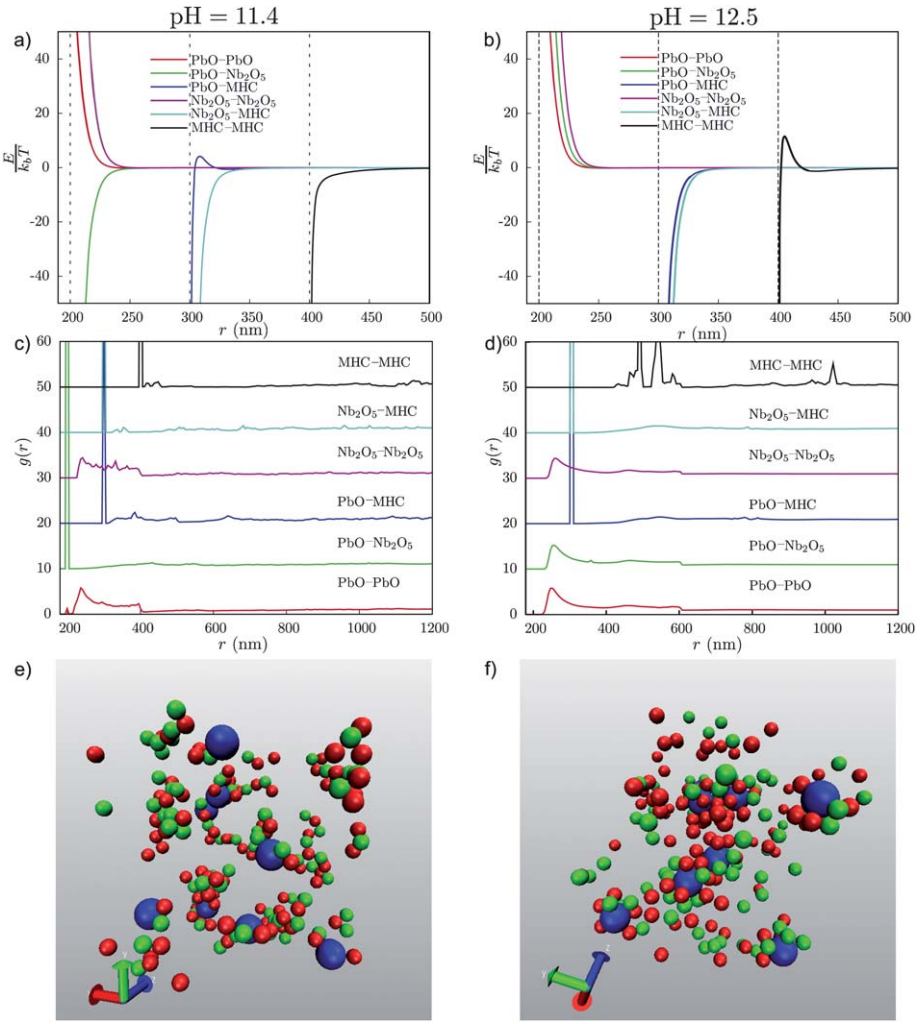

Fig. 6 Results for bigger MHC particles. (a and b) Interaction potentials between six pairs of particles in the suspension. (c and d) Simulated radial distribution functions for the pairs of particles. (e and f) Snapshots of equilibrated spatial distribution of particles in the suspensions. Color code same as above (PbO is colored red, Nb_2O_5 green, and MHC blue). Perspective 3D views are generated with VMD program.[29] The results for the pH 11.4 sample are presented on the left and for the pH 12.5 sample on the right.

close contact during the drying process of the perovskite synthesis.

To further judge the effects of the size of the MHC particles, the results of the pH 12.5 sample are compared for the three cases (*i.e.*, MHC of equal size as other two types, smaller MHC, and bigger MHC), corresponding to the Fig. 3, 5, and 6. There is no change in the type of pair interactions, in all the cases four repulsive and two attractive interactions are present. However, the distance at which these interactions are active is changed when the size of MHC particles is changed. The difference is in the steric effect, which influences the equilibrium distribution of the particles in the suspension. Due to the smaller size, the number of MHC particles is higher in the case of smaller MHC particles, and thus several MHC particles are adsorbed to one PbO or Nb_2O_5 particle, thus sterically preventing the contacts between PbO and Nb_2O_5. In the case of equal-sized particles, the situation is that several PbO and Nb_2O_5 particles adsorb to one MHC particle. In the case of bigger size of MHC particles, even more PbO and Nb_2O_5 particles are adsorbed on one MHC particle, while more than 50% of them are not adsorbed. The effect of sterically preventing the contacts between the PbO and Nb_2O_5 is thus more pronounced when the MHC particles are of smaller size and their number is larger (to keep the same volume fraction).The simulation results imply that in the case where the MHC particles are smaller, the structure of clusters can be even more favorable for the perovskite formation. This further suggests that smaller MHC particles should be preferably used in the experiments or need to be pre-milled to reduce their size.

4.3 Direct contacts between reagent particles in the suspension

For efficient solid-state reactions direct contacts between the reacting particles are crucial. As it is explained above, for a multicomponent system not all such contacts are beneficial. In our three-component system six possible contacts are PbO–PbO, Nb_2O_5–Nb_2O_5, MHC–MHC, PbO–Nb_2O_5, PbO–MHC, and Nb_2O_5–MHC contacts. Direct contacts between PbO–MHC and Nb_2O_5–MHC are desired for the solid-state reaction in the

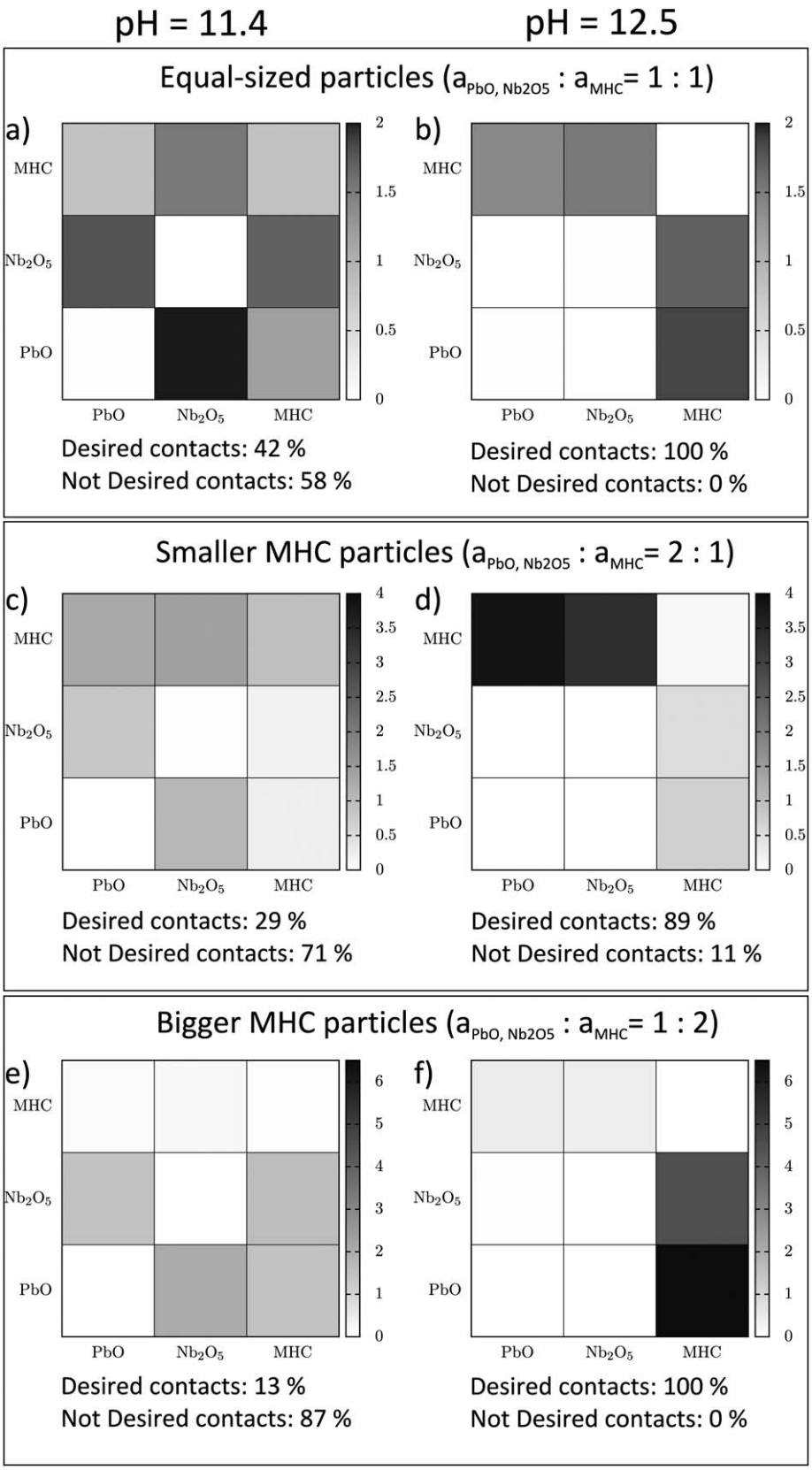

Fig. 7 Number of direct contacts per particle between the reagent particles in our system calculated from the equilibrated distributions of particles. The color of the matrix cell represents the number of contacts between particles rows and columns normalized per number of particles in the columns. The results for the pH 11.4 sample are presented on the left and for the pH 12.5 sample on the right. The results for equal-sized particles are presented in the first row a) and b), for smaller MHC particles in the second row c) and d), and for the bigger MHC particles in the third row e) and f).

perovskite synthesis.[5] However, the PbO–Nb_2O_5 direct contacts need to be avoided, because they promote the formation of secondary pyrochlore phase. The contacts between the same type of particles, *i.e.*, PbO–PbO, Nb_2O_5–Nb_2O_5, and MHC–MHC are also not desired. In the simulations we analyze the number of direct contacts between different pairs of particles in the aggregates, that are formed at different pH conditions and particle sizes. The number of contacts per particle is calculated for the equilibrium distributions of particles. The results are presented in the matrices in Fig. 7. Each matrix cell represents the number of contacts between two corresponding types of particles in the aggregate. The contacts are normalized per number of particles presented in the columns. For example in Fig. 7a the color of the matrix cell Nb_2O_5–PbO corresponds to the contacts between PbO and Nb_2O_5 normalized per number of PbO particles in the simulation box. The result is 1.4, which shows that there are on average 1.4 Nb_2O_5 particles in direct contact with one PbO particle in the case of equal-sized particles at pH = 11.4. The PbO particles are also in direct contact with MHC, but less then 0.5 MHC are on average connected with one PbO. The Nb_2O_5 particles are in direct contact with 1.8 PbO and 1 MHC particles on average. MHC particles are in direct contact with all three species *i.e.*, PbO, Nb_2O_5, and MHC. The ratio between the desired, *i.e.*, PbO–MHC, Nb_2O_5–MHC, and not desired, *i.e.*, PbO–PbO, Nb_2O_5–Nb_2O_5, MHC–MHC, PbO–Nb_2O_5, direct contacts is also presented in the Figure. For the pH 11.4 case, with equal-sized particles, the 42% of contacts are desired and 58% are not desired. On the contrary pH 12.5 sample, with equal-sized particles (Fig. 7b), contains only desired contacts. Both PbO and Nb_2O_5 are in contact with approximately one MHC particle. One MHC particle is on average in contact with 1.5 PbO particles and 1.2 Nb_2O_5 particles.

The second row in Fig. 7 presents the results for the systems with smaller MHC particles. At pH = 11.4 almost one Nb_2O_5 particle is in direct contact with one PbO particle, more then one PbO particle is in contact with one Nb_2O_5, and also one MHC particle is in direct contact with one MHC. These are not desired contacts which account for more than 70% of all contacts in the system. But desired PbO–MHC, and Nb_2O_5–MHC contacts are also present in the suspension. The opposite result is again observed at pH = 12.5, where almost 90% of contacts are the desired ones. Almost 4 MHC particles are in contact with one PbO at pH = 12.5, whereas at pH = 11.4 this value is only 1.3. Similarly there are 3.4 MHC particles in contact with one Nb_2O_5 at pH = 12.5, and only 1.4 at pH = 11.4. Smaller amount of not desired MHC–MHC direct contacts is observed at pH = 12.5 in comparison to pH = 11.4.

The case with bigger MHC particles is presented in the last row of Fig. 7. Again there are almost 90% of all contacts at pH = 11.4 which are not desired, whereas at pH = 12.5 only the desired contacts are present. At the lower pH the majority of contacts are of the PbO–Nb_2O_5 type and there are some PbO–MHC and Nb_2O_5–MHC contacts present. Whereas at the higher pH only PbO–MHC and Nb_2O_5–MHC contacts are present. In this case one MHC particle is in direct contact with 6.5 PbO particles and 4.5 Nb_2O_5 particles on average.

If we compare only the pH 12.5 samples with different sizes of MHC particles, we can observe that the size and consequently the number of MHC particles, have a major influence on the number of a certain type of direct contacts. For example one PbO particle is in direct contact with a different number of MHC particles at different conditions. The smaller size of MHC particles enables a higher number of MHC particles in contact with either one PbO or one Nb_2O_5. This enables an effective steric hindrance for the formation of PbO–Nb_2O_5 contacts, which is beneficial for the solid–state reaction.

In summary of the statistics of direct particle contacts, we can conclude that the higher pH and the smaller size of MHC particles make the conditions which are preferable for the solid-state reaction.

5 Conclusions

Within the MC simulations in this work we have investigated the formation of clusters of charged colloidal particles of the reagent powders—lead oxide, magnesium hydroxy carbonate (MHC), and niobium oxide—in the aqueous suspensions with the conditions corresponding to the experiment of ref. 5. Our focus has been to investigate the spatial distributions of the reagent particles that arise through the aggregation in the aqueous suspension, which is relevant in view of the subsequent solid-state reactions for the PMN synthesis.

In close relation with the experimental parameters, in particular the zeta potentials and volume fractions of the reagent particles, our numerical simulations have revealed that different types of clusters are energetically favored at different pH of the suspensions, which are used in the experiment. Specifically, at pH = 11.4 a large population of the precursor clusters in which close contacts between PbO and Nb_2O_5 is achieved. Thus the secondary pyrochlore phase can be formed in the subsequent solid-state reaction between these particles, as found in the experiment. On the contrary, at higher pH = 12.5, zeta potentials of the reagent particles change such that the nature of the attraction–repulsion potentials between these pairs of particles is altered. The resulting equilibrium clusters contain the reagent particles PbO and Nb_2O_5 effectively separated by the MHC particles. The situations of equal-size of all reagent particles (as in the real experiment) and the numerically investigated situation with smaller MHC particles are particularly favorable for this type of clusters, from which then the pure perovskite phase can form.

For the purpose of this work we kept the parameters of the model as close to the experiment as possible and investigated the cluster formation of the precursor particles, which is relevant for the experiment. The parameters stemming from the pH values of the suspension and particle sizes have been varied in the simulations. Within the model and the MC methods, the values of other parameters can also be varied. For instance, the volume fraction of different reagent particles can be varied in a much wider range, which can be relevant for analysis of the cluster–cluster aggregation processes. This is left for future study.

In summary, we have shown how the computer simulations, based on suitable models and realistic parameters, can help to unravel the processes which occur at the particle level in the synthesis of the PMN ceramics. With such information at hand, it is possible to improve the parameters for future experiments in the production of higher quality materials.

Acknowledgements

The authors would like to acknowledge the contribution of prof. Barbara Malič and would like to thank J. Cilenšek, E. Ion, S. Glinšek and S. Drnovšek for the help with experimental work. This work was supported by the Slovenian Research Agency (Project number: PR-02485 and P2-105). B.T. thanks the support from the national program P1-0044 (Slovenia).

References

1 G. H. Heartling, *J. Am. Ceram. Soc.*, 1999, **82**, 2341–2359.
2 T. R. Shrout and A. Halliyal, *Am. Ceram. Soc. Bull.*, 1987, **66**, 704–711.
3 *Piezoelectric materials in devices*, ed. N. Setter, EPFL, Lausanne, Switzerland, 2002.
4 H. Uršič, M. Hrovat, J. Holc, M. S. Zarnik, S. Drnovšek, S. Maček and M. Kosec, *Sens. Actuators, B*, 2008, **133**, 699–704.
5 G. Trefalt, B. Malič, D. Kuščer, J. Holc and M. Kosec, *J. Am. Ceram. Soc.*, 2011, DOI: 10.1111/j.1551-2916.2011.04443.x.
6 S. L. Swartz, T. R. Shrout, W. A. Schultze and L. E. Cross, *J. Am. Ceram. Soc.*, 1984, **67**, 311–314.
7 K. R. Han and S. Kim, *J. Mater. Sci.*, 2000, **35**, 2055–2059.
8 J. M. Lopéz-Lopéz, M. Puertas, A. Moncho-Jordá, A. Schmitt and R. Hidalgo-Álvarez, *Soft Matter*, 2010, **6**, 3568–3572.
9 M. Hütter, *Phys. Chem. Chem. Phys.*, 1999, **1**, 4429–4436.
10 M. Cerbelaud, A. Videcoq, P. Abélard, C. Pagnoux, F. Rossignol and R. Ferrando, *Langmuir*, 2008, **24**, 3001–3008.
11 M. Cerbelaud, A. Videcoq, P. Abélard, C. Pagnoux, F. Rossignol and R. Ferrando, *Soft Matter*, 2010, **6**, 370–382.
12 J. Liu and E. Luijten, *Phys. Rev. E: Stat., Nonlinear, Soft Matter Phys.*, 2005, **72**, 061401.
13 M. Dijkstra, *Curr. Opin. Colloid Interface Sci.*, 2001, **6**, 372–382.
14 J. C. Chen and A. S. Kim, *Adv. Colloid Interface Sci.*, 2004, **112**, 159–173.
15 D. Frenkel and B. Smit, *Understanding Molecular Simulation*, Academic Press, San Diego, 2002.
16 M. P. Allen and D. J. Tildesley, *Computer Simulation of Liquids*, Claredon Press, Oxford, 1989.
17 M. Blunt, A. Stannard, E. Pauliac-Vaujour, C. Martin, I. Vancea, M. Šuvakov, U. Thiele, B. Tadić and P. Moriarty, in *The Oxford Handbook of Nanoscience and Technology*, Oxford University Press, 2010, vol. I, ch: Patterns and Pathways in Nanoparticle Self-Organization.
18 J. M. Lopéz-Lopéz, A. Schmitt, A. Moncho-Jordá and R. Hidalgo-Álvarez, *Soft Matter*, 2006, **2**, 1025–1042.
19 L. Hong, A. Cacciuto, E. Luijten and S. Granick, *Langmuir*, 2008, **24**, 621–625.
20 S. Kim, K.-S. Lee, M. R. Zachariah and D. Lee, *J. Colloid Interface Sci.*, 2010, **344**, 353–361.
21 S. Diez Orrite, S. Stoll and P. Schurtenberger, *Soft Matter*, 2005, **1**, 364–371.
22 E. Bianchi, P. Tartaglia, E. Zaccarelli and F. Sciortino, *J. Chem. Phys.*, 2008, **128**, 144504.
23 B. V. Derjaugin and L. Landau, *Acta Physicochim. URSS*, 1941, **14**, 633–662.
24 E. J. Verwey and J. T. G. Overbeek, *Theory of the stability of lyophobic colloids*, Elsevier, Amsterdam, 1948.
25 M. Elimelech, J. Gregory, X. Jia and R. A. Williams, *Particle Deposition and Aggregation*, Butterworth–Heinemann, Oxford, 1998.
26 L. Bergström, *Adv. Colloid Interface Sci.*, 1997, **70**, 125–169.
27 R. Hogg, T. W. Healy and D. W. Fuerstenau, *Trans. Faraday Soc.*, 1966, **62**, 1638–1651.
28 D. Heermann, *Computer Simulation Methods in Theoretical Physics*, Springer-Verlag, Berlin, 1990.
29 W. Humphrey, A. Dalke and K. Schulten, *J. Mol. Graphics*, 1996, **14**, 33–38.